RUSSIAN JOURNAL OF ELECTROCHEMISTRY, 2025, Vol. 61, No. 1, pp. 71–79

CONSOLIDATION OF Al AND Ta-SUBSTITUTED $Li_7La_3Zr_2O_{12}$ POWDERS WITH LITHIUM–ION CONDUCTIVITY BY SPARK PLASMA SINTERING [1]

© 2025 G. B. Kunshina[a, *], I. V. Bocharova[a], A. A. Belov[b], O. O. Shichalin[b], E. K. Papynov[b]

[a]Tananaev Institute of Chemistry, Subdivision of the Federal Research Centre "Kola Science Centre of the Russian Academy of Sciences", Apatity, Russia

[b]Far Eastern Federal University, Vladivostok, Russia

[*]e-mail: g.kunshina@ksc.ru

Received: July 02, 2024
Revised: October 18, 2024
Accepted: October 28, 2024

Abstract. Monophase powders of cubic modification with nominal composition $Li_{6.4}Al_{0.2}La_3Zr_2O_{12}$ (Al-LLZO) and $Li_{6.52}Al_{0.08}La_3Zr_{1.75}Ta_{0.25}O_{12}$ (Ta-LLZ) were synthesized. Dense (~97–98%) ceramic samples of solid electrolyte with increased stability in air were obtained from these powders by spark plasma sintering. High Li-ion conductivity parameters ($4–6\times10^{-4}$ S/cm) meeting to the world standard have been achieved.

Keywords: *solid electrolyte, lithium lanthanum zirconate, spark plazma sintering, cubic modification ionic conductivity*

DOI: 10.31857/S04248570250105e4

INTRODUCTION

In the last decade, inorganic solid electrolytes with high Li^+ ion conductivity have been intensively studied in order to use them as membranes, composite electrodes, and electrolytes in solid-state electrochemical devices [1, 2]. Solid electrolytes have a number of advantages over liquid and polymer materials, as they are characterized by high mechanical strength, chemical and thermal stability. The use of solid electrolytes can significantly increase the safety of lithium-ion batteries (LIB) [3]. Substituted lithium titanophosphates and germanophosphates with the NASICON structure, solid solutions based on lithium-lanthanum titanates with the perovskite structure, and representatives of a new family of lithium-conducting solid electrolytes with the garnet structure of the composition $Li_{7-3x}Al_xLa_3Zr_2O_{12}$ are considered promising in terms of ion conductivity and stability [4].

The structure of $Li_7La_3Zr_2O_{12}$ garnet has two crystal modifications: tetragonal and cubic. Tetragonal $Li_7La_3Zr_2O_{12}$ contains a fully ordered Li^+ distribution and crystallizes in the $I41/acd$ space group. Cubic $Li_7La_3Zr_2O_{12}$ crystallizes in the $Ia\bar{3}d$ space group and exhibits a disordered distribution of lithium ions and vacancies caused by lithium deficiency. The lithium-ion conductivity of the tetragonal modification is two orders of magnitude lower than that of the cubic one. The cubic modification can be stabilized by partial cationic substitution, for which the solid electrolyte $Li_7La_3Zr_2O_{12}$ is doped with ions Al^{3+}, Ga^{3+}, Nb^{5+}, Ta^{5+}, etc. The largest number of studies are devoted to the partial replacement of Li^+ with Al^{3+}, which is an inexpensive alloying additive and can also be inadvertently introduced into the garnet structure during annealing in corundum crucibles. However, the Al^{3+} ion blocks lithium positions, which leads to a decrease in Li^+ concentration and a slowdown in Li^+ diffusion (unlike Ta^{5+}, which is used to replace Zr^{4+} to avoid a decrease in Li+ content).

We synthesized powders of Al-substituted $Li_7La_3Zr_2O_{12}$ **(Al-LLZO)** of cubic modification by melting the charge followed by solid-phase annealing, which consists in the interaction of charge components consisting of low-melting crystallohydrates $ZrO(NO_3)_2{\cdot}2H_2O$, $La(NO_3)_3{\cdot}6H_2O$ and $Al(NO_3)_3{\cdot}9H_2O$ [5–7]. The powders were pressed into tablets without binding components in a mold with a diameter of 12 mm with a force of 100 MPa and sintered in air at a temperature of 1100–1150° C in a program-controlled MIMP-3 muffle under a mother powder of the same composition. For further practical use, it is necessary to obtain samples with maximum density from these powders. As noted in these papers, it was not possible to obtain dense

[1] Based on the materials of the report at the 17th International Meeting "Fundamental and applied problems of solid state ionics", Chernogolovka, June 16–23, 2024.

Table 1. Modes of solid-phase sintering of Al-LLZO tablets

I stage (heating rate, 10 degr./min.)		II stage (heating rate 2 degr./min)			Total heat treatment time, h	ρ,%
t, °C	Heating time, min	t, °C	Heating time, min	Hold, h		
20–1100	110	1100–1150	25	4	6	75
				6	8	76–78
20–1050	105	1050–1100	25	8	10	72
		1050–1150	50	6	8.5	79
		1050–1150	50	8	10.5	76–77
20–1000	100	1000–1100	50	8	10.5	74–79
				12	14.5	76–77
20–1200	180	1200		7	10	80
20–900	90	900–1150	125	8	11.5	74
		900–1200	150	8	12	73–74

samples using the classical method of high-temperature 2-stage sintering with prolonged exposure (Table 1).

The maximum density did not exceed 80% (even with the use of preliminary mechanical activation of powders on the AGO-2C centrifugal planetary mill). At the same time, only dense Al-LLZO ceramics increase the overall ionic conductivity and prevent lithium dendrites from penetrating through the pores during cycling, which can lead to a short circuit or destruction of the sample [8, 9]. In addition, Al-LLZO ceramic samples with low density are unstable when stored in air under normal conditions [10–13]. In this regard, it is necessary to obtain samples with maximum density.

To increase the density of solid electrolytes by solid-phase sintering, various sintering additives (Li_2CO_3, Li_3PO_4, $LiBO_2$, LiOH, LiCl, LiF, $Li_2B_4O_7$) are used, which contribute to the compaction of samples, improve the microstructure, which leads to a decrease in grain boundary resistance and an increase in ionic conductivity [14]. However, sintering additives partially induce the formation of small amounts of amorphous phases in the grain boundary regions. The formation of secondary phases limits the ionic conductivity of the material [15].

An innovative spark plasma sintering (**SPS**) method, which consists in high-speed consolidation of dispersed materials of various chemical and fractional compositions due to electrical pulse heating during mechanical compression, may be promising for obtaining solid electrolytes with maximum density [16, 17]. The absence of sintering additives and plasticizers, as well as the short cycle time of single-stage sintering (minutes) to achieve maximum material density (up to 100% of the theoretical) are the advantages of the SPS method over traditional sintering technologies. Despite the fact that the SPS method is a high-tech approach in a new generation of ceramic synthesis and is a global trend in the creation of modern ceramic materials for functional purposes, it is rarely used to consolidate solid electrolytes [18–22].

We have demonstrated the positive experience of using the IPS method to obtain a solid electrolyte with a NASICON structure of composition $Li_{1.3}Al_{0.3}Ti_{1.7}(PO_4)_3$ in [23]. From powders $Li_{1.3}Al_{0.3}Ti_{1.7}(PO_4)_3$ (LATP) with a narrow granulometric composition, high-density lithium-conductive ceramics (~97–98%) were obtained by SPS method under optimal technological conditions (sintering temperature 900 °C, molding pressure 50 MPa, sintering duration 5 min). There was no change in the phase composition of the LATP samples during the SPS process. The use of the SPS method made it possible to significantly reduce the consolidation time, reduce the sintering temperature, and achieve an increase in the density and ionic conductivity of LATP ceramics. The maximum ionic conductivity (σ total = 2.9×10^{-4} S/cm and σ bulk = 1.6×10^{-3} S/cm) is achieved for single-phase LATP samples in combination with the maximum density (97–98%). This is significantly higher than the results presented by the authors [24].

The purpose of this work was to develop a method for obtaining dense samples of Al- and Ta-doped solid electrolyte $Li_7La_3Zr_2O_{12}$ with high ionic conductivity by the SPS method for use in new-generation lithium batteries (fully solid-state, lithium-sulfur and lithium-air batteries).

Table 2. Modes of preparation of initial powders of cubic modification Al-LLZO and Ta-LLZO and subsequent consolidation by SPS method

	I stage			II stage			III stage				SPS				
	t, °C	τ, h	XRF	t, °C	τ, h	XRF	MA	t, °C	τ, h	XRF	t, °C	τ, min	XRF	ρ, g/cm^3	σ, S/cm
Al-LLZO	900	4	t-LLZO, c-LLZO	–			–				1000	10	t-LLZO, c-LLZO	89–90%	$1\cdot10^{-5}$
	900	4	t-LLZO, c-LLZO	1000	4	t-LLZO, c-LLZO	4x1 min	1000	4	c-LLZO	1000	10	c-LLZO	4.9 (96%)	$4\cdot10^{-4}$
Ta-LLZO	900	4	t-LLZO, c-LLZO, La_2O_3, ZrO_2, Ta_2O_5	1000	4	t-LLZO, c-LLZO	–	1100	6	c-LLZO	1100	15	c-LLZO	5.18 (98%)	$6\cdot10^{-4}$

EXPERIMENTAL PART

Preparation of Al-LLZO and Ta-LLZO powders

Monophase powders of Al-substituted solid electrolyte $Li_7La_3Zr_2O_{12}$ of nominal composition $Li_{6.4}Al_{0.2}La_3Zr_2O_{12}$ (Al-LLZO) were prepared as described in [5]. Mechanical activation (**MA**) after powder annealing at 900 °C for 4 hours was carried out in an AGO-2C planetary mill in a 4x1 min mode with a centrifugal factor of 20 g in drums, the inner surface of which is made of zirconium dioxide, using balls of the same material [25]. The balls: load mass ratio is 20:1. In order to ensure the macro uniformity of the powders, the mill was switched off every 1 min and the contents of the drums were mixed with a spatula. Next, the mechanically activated powder was calcined at a temperature of 1000 °C (heating rate of 10 degrees /min) for 4 hours.

Monophase powders of Ta-substituted solid electrolyte Li7La3Zr2O12 of nominal composition $Li_{6.52}Al_{0.08}La_3Zr_{1.75}Ta_{0.25}O_{12}$ **(Ta-LLZO)** were prepared as described in [26]. Since substitution with Ta ions ensures the transition of the tetragonal modification to a cubic one under milder conditions than when substituting with Al ions, mechanical activation of Ta-LLZO powders was not performed. The authors [27] conducted all experiments to study the chemical and thermal stability of Ta-LLZO after SPS using commercial $Li_{6.4}La_3Zr_{1.4}Ta_{0.6}O_{12}$ [28].

Consolidation of Al-LLZO and Ta-LLZO powders by SPS method

The consolidation of the prepared Al-LLZO and Ta-LLZO powders by the SPS method was carried out at the Spark Plasma Sintering System SPS-515S installation (Dr. Sinter·LAB™, Japan) according to the scheme: 1.5 g of LLZO powder was placed in a graphite mold (working diameter 1.25 mm), pressed (pressure 20.7 MPa), then the blank was placed in a vacuum chamber (10^{-5} atm) and sintered. Graphite foil with a thickness of 200 microns was used to prevent the consolidated powder from baking to the mold and plungers, as well as for unhindered extraction of the resulting sample. SPS consolidation of LLZO powders was carried out at a pressure of 50 MPa with a heating rate of 50 °C/min in the range of 900–1100 °C with exposure for 5–15 minutes.

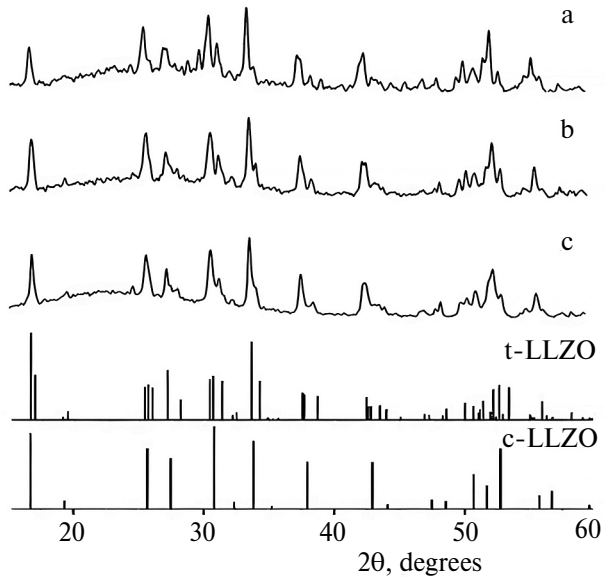

Fig. 1. Diffractograms of Al-LLZO powder after solid-phase annealing at 900 °C (a) and 1100 °C (b) and after SPS at 1000 °C for 10 min (c).

The synthesized solid electrolytes Al-LLZO and Ta-LLZO were characterized by X-ray phase analysis (**XRF**), energy dispersive X-ray spectroscopy (**EDX**), and impedance spectroscopy. Phase analysis was performed using an XRD-6000 and Rigaku MiniFlex-600 diffractometer, CuKα radiation, scattering angle range $2\theta = 10–70^o$. Data processing by the Rietveld method (refinement of lattice parameters)

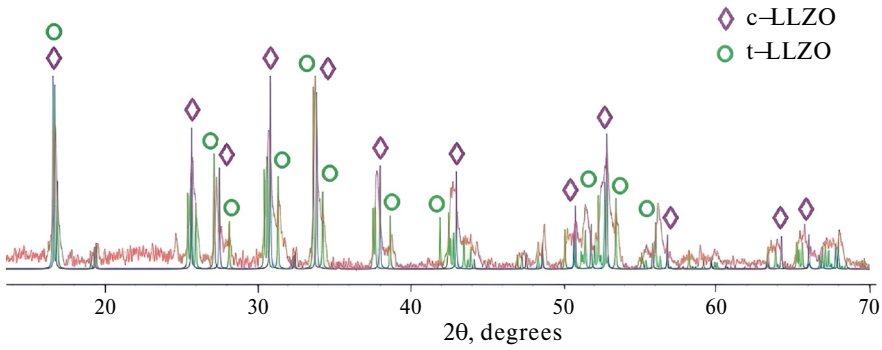

Fig. 2. Diffractograms of Al-LLZO powder after SPS at 1000 °C for 10 min.

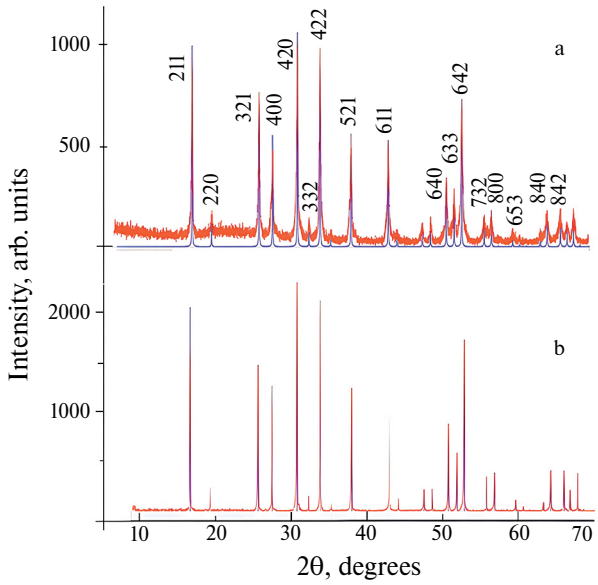

Fig. 3. Diffractograms of mechanically activated Al-LLZO powder of cubic modification (a) after annealing at 1000 °C and (b) subjected to SPS.

was performed using the smartLAB Studio II software within the Rigaku MiniFlex-600 diffractometer. The international database ICDD PDF-4 was used to decipher diffractograms.

The density of the samples was determined by hydrostatic weighing (on an LV-210A electronic scale with an accuracy of 0.001 g) using CCl_4 as an immersion liquid. The theoretical (radiographic) density for Al-LLZO was 5.1 g/cm^3 (ICDD 01–080–7219), and for Ta-LLZO it was 5.26 g/cm^3 (ICDD 04–023–7624).

Ion conductivity (σ) was studied by electrochemical impedance spectroscopy [29] with an AC signal amplitude of 0.1 V using a Z-2000 impedance meter (Elins). The measurements were carried out using a two-electrode circuit in a shielded cell of a clamping structure with graphite electrodes. The frequency range of measurements was 10^2–2×10^6 Hz. The specific ionic conductivity (σ_{total}) was calculated taking into account the geometric dimensions according to the formula:

$$\sigma_{total} = \frac{4h}{R\pi d^2}, \quad (1)$$

where R is the resistance of the tablet, determined based on the analysis of the impedance spectrum, h and d are the height and diameter of the tablet, respectively.

The electronic conductivity was determined by potentiostatic chronoamperometry (**PCA**), recording the current density as a function of time after switching on the polarizing potential [9] using a P-8 potentiostat (Elins, Russia). The value of the electronic conductivity of Ta-LLZO was calculated using the formula:

$$\sigma_e = \frac{I_{st}h}{US}, \quad (2)$$

where I_{st} is the stabilization current, U is the applied DC voltage, and h and S are the height and cross-sectional area of the tablet, respectively.

RESULTS AND DISCUSSION

According to the results of XRF, it was established (Fig. 1*a*), that after the 1st stage of Al-LLZO synthesis, as a result of annealing at 900 °C for 4 hours, a product with a garnet structure containing no initial unreacted substances and non-conductive impurity phases (La_2O_3, ZrO_2, $La_2Zr_2O_7$) was formed. The samples are well-crystallized powders of individual Al-LLZO in the form of a mixture of 2 modifications: tetragonal (ICDD PDF 01–080–6140) and cubic (ICDD PDF 01–080–7219) in commensurate quantities. An increase in temperature (up to 1100 °C) and the duration of powder annealing (up to 6 hours) did not provide a pure cubic modification of Al-LLZO, and a mixture of tetragonal and cubic modifications was also present on the X-ray image (Fig. 1*b*).

Initially, Al-LLZO powders obtained after annealing at 900 °C were used for SPS consolidation. According

Table 3. Al-LLZO lattice parameters determined by the Rietveld method

Sample	$a = b = c$, Å	Rp,%	Rwp,%	χ^2	V, Å^3
Al-LLZO	12.9735	10.57	13.47	2.1449	2185
Al-LLZO after SPS	12.96052	3.04	4.13	2.1934	2177
Al-LLZO [30]	12.96529	2.895	4.105	2.099	2179

to the XRF data, at various SPS modes (sintering temperature 900–1000 °C, molding pressure 50 MPa, sintering duration 5–10 min), Al-LLZO tablets were also obtained as a mixture of 2 modifications (Fig. 2). In this regard, the ionic conductivity measured by electrochemical impedance spectroscopy was insignificant (it was at the level of 1×10^{-5} S/cm). Apparently, the short-term SPS process does not ensure the complete transformation of the low-conducting tetragonal modification of Al-LLZO into a cubic one. When using the tetragonal modification, the authors [21] needed additional heat treatment for 12 hours at 1175 °C of LLZO samples subjected to SPS, since the total ionic conductivity of LLZO samples after SPS was only 7×10^{-6} S/cm.

Many researchers have encountered the problem of the formation of a non-conductive impurity phase $La_2Zr_2O_7$ after the consolidation of the solid electrolyte LLZO by the SPS method [18–22]. In this regard, the data obtained in a recent paper [22] seem contradictory, where the authors claim a high ionic conductivity with a cubic modification of LLZO in the sample at the level of 84% and a non-conducting impurity phase $La_2Zr_2O_7$ at the level of 13%. Obviously, for the SPS method, powders of a purely cubic modification must be synthesized as the initial LLZO powder, as the authors [19] do, who ground the initial $LiOH\cdot H_2O$, La_2O_3, ZrO_2 and Ta_2O_5 in a ball mill with isopropyl alcohol for 12 hours. After drying, the powder was calcined at 900 °C for 6 hours, then crushed, dried under the same conditions, and heated at 1100 °C for 12 hours in the 2nd stage. The powder was then re-ground, pressed into tablets, and sintered at 1130 and 1230 °C for 36 hours to obtain a cubic structure electrolyte [19]. The listed processing operations are lengthy, labor-intensive and energy-consuming.

We have optimized the transition from tetragonal modification to cubic modification using mechanical activation. As a result of MA, the dispersion and reactivity of the powders increases and the tetragonal modification of Al-LLZO is completely transformed into a cubic one after annealing at 1000 °C (Fig. 3*a*).

Subsequent SPS consolidation of Al-LLZO and Ta-LLZO powders of purely cubic modification (obtained according to Table 2) led to the formation of tablets with a density of ~96–98% of the theoretical. At the same time, the structure of the cubic modification

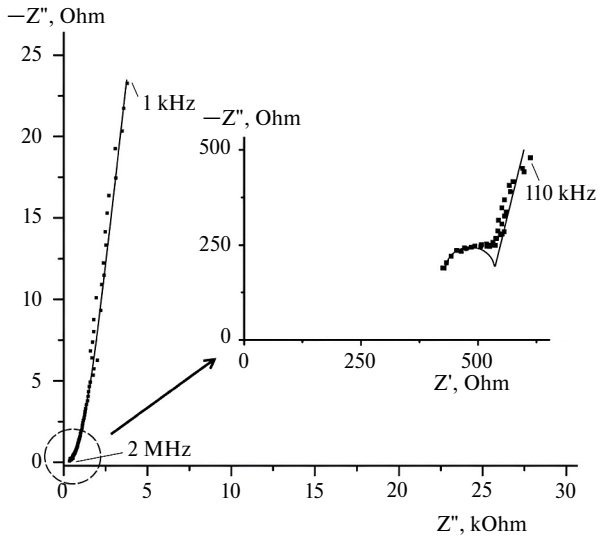

Fig. 4. The spectrum of the Ta-LLZO electrochemical impedance after SPS in the range of 10^3–10^6 Hz. The insert has a high-frequency section (10^5–10^6 Hz).

($Ia\bar{3}d$ space group) was preserved and the peak intensity increased significantly, which indicates an increase in the crystallinity of the samples after SPS (Fig. 3*b*). It should be emphasized that it was not possible to obtain samples of the specified density using the multi-stage classical solid-phase sintering of powders with prolonged exposure, especially for Ta-LLZO [26].

For monophase Al-LLZO powders obtained after annealing at 1000°C, as well as Al-LLZO samples subjected to SPS, Rietveld analysis was performed. The lattice parameters of cubic Al-LLZO were calculated by the method of full-profile analysis of WPPF (Whole Powder Pattern Fitting) radiographs. The R-factor criteria were the values of the profile R-factors Rp and Rwp, calculated using standard formulas (Table 3). The values of the WPPF parameters, commonly used to assess the quality of profile fitting, confirm the good quality of the results obtained. The WPPF refinement showed that the structure of the samples corresponds to the cubic phase with the $Ia\bar{3}d$ space group.

Fig. 4 shows the spectrum of the electrochemical impedance of a Ta-LLZO tablet subjected to SPS. The impedance hodographs of the Ta-LLZO and Al-LLZO samples constructed on the complex plane $Z''=f(Z')$ are identical and consistent with the results

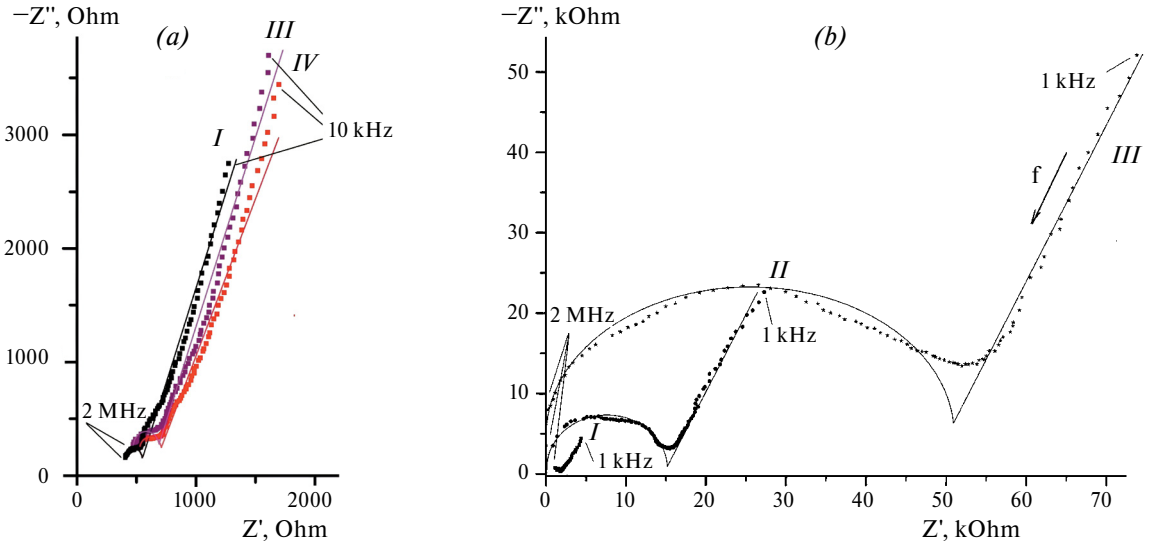

Fig. 5. Impedance hodographs of Ta-LLZO samples after SPS (*a*) and after solid-phase sintering (*b*). *I* – measured immediately after synthesis, *II* – after 10 days, *III* – after 1 month, *IV* – after 2 months of storage in air.

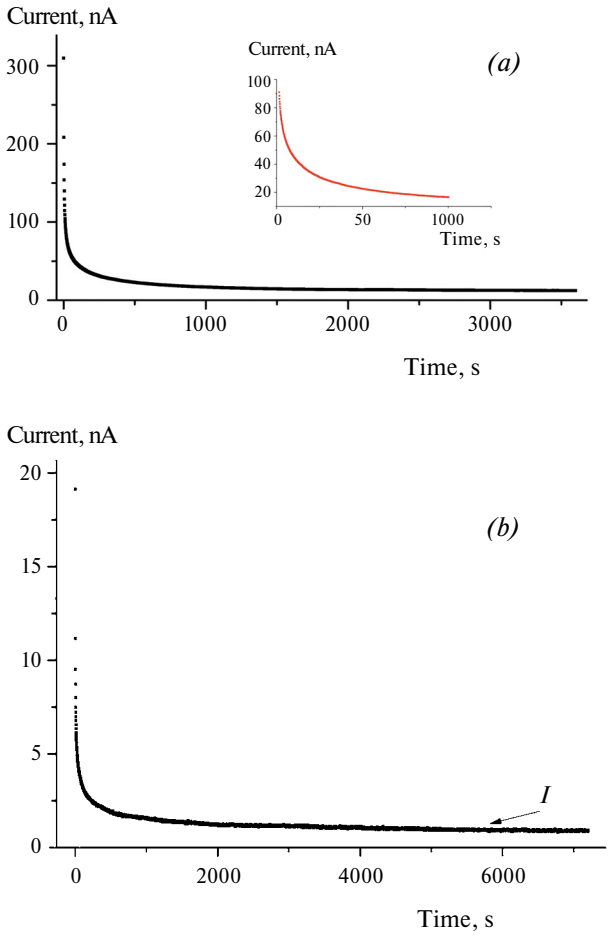

Fig. 6. Chronoamperometric curves for Ta-LLZO after solid-phase sintering (a) and after SPS (b).

of the authors [20, 31–33], who conclude that the impedance of the grain boundaries is negligible compared to the impedance of the grains, probably due to almost complete absence of grain-boundary resistance. The conductivity value was calculated by extrapolating the high-frequency section of the hodograph onto the active resistance axis. The value of the specific total ionic conductivity (σ_{total}) of Ta-LLZO tablets at 20 °C, calculated by formula (1), was 6×10^{-4} S/cm and 6 times higher than the value measured on Ta-LLZO tablets with a low density (69%), previously obtained by solid-phase sintering [26]. The value of the total ionic conductivity of Al-LLZO tablets at room temperature was 4×10^{-4} S/cm, which corresponds to the maximum values given by most researchers [34] and is twice higher than the value of the ionic conductivity of Al-LLZO tablets with a density of 75–85%, obtained earlier by solid-phase sintering [6–7]. This confirms the conclusion that the main factors influencing the ionic conductivity of Al-LLZO and Ta-LLZO are the absence of impurity phases, highly conductive cubic modification, and maximum sample density [35].

As noted [5], LLZO samples are unstable when stored in air under normal conditions due to the formation of nonconducting phases: Li_2CO_3 (on the surface of the tablets) and $La_2Zr_2O_7$ (in volume) due to reaction with H_2O and CO_2. The kinetics of hydration and carbonation of Ta-LLZO powders has recently been studied in [36]. It has been established that the rate of the hydration and carbonation reactions strongly depends on the particle size and, consequently, on the surface area. For Al-LLZO tablets with a porosity of 17%, it was found that spontaneous

cracking and a decrease in ionic conductivity by 3 orders of magnitude occur after three weeks of storage [13]. The process of Li_2CO_3 formation is reversible, since upon repeated annealing of the LLZO tablet at a temperature of 900°C, the conductivity value practically returned to the initial result [5].

A distinctive feature of the Al-LLZO and Ta-LLZO tablets consolidated by the SPS method (density ~96–98%) is increased air stability. As follows from Fig. 5*a*, the ionic conductivity of Ta-LLZO samples remained almost unchanged after long-term storage under normal conditions (for 2 months). For comparison, as a result of storage of Ta-LLZO tablets (with a density of 68–70%) after solid-phase sintering for one month, the ionic conductivity decreased by 2 orders of magnitude and amounted to 3×10^{-6} S/cm (Fig. 5*b*). Achieving good storage stability is an important prerequisite for the practical use of solid electrolytes with a garnet structure.

The ideal solid electrolyte should be a purely ionic conductor, since electronic conductivity causes an electrical leak or short circuit in the LIB. High electronic conductivity may be responsible for the formation of dendrites in solid electrolytes [9]. A critical requirement for solid electrolytes is considered to be high ionic conductivity $>10^{-4}$ S/cm. Low electronic conductivity should be another criterion for solid electrolytes regarding their practical use [9]. The electronic conductivity of Ta-LLZO was evaluated by the PCA method [37]. A constant voltage of 1 V from the potentiostat was applied to a symmetrical cell C/Ta-LLZO/C with blocking graphite electrodes. The steady-state current was set for 1–2 hours. The polarization chronoamperometric curves of Ta-LLZO obtained by solid-phase sintering and the SPS method are shown in Fig. 6.

The chronoamperometric curves are identical and the value of the electronic conductivity is almost the same, since the electronic conductivity depends less on the density of the sample, but is determined mainly by the deviation from stoichiometry and the presence of uncontrolled impurities in the solid electrolyte. The value of the electronic conductivity σ_e Ta-LLZO did not exceed 10^{-9} S/cm, which is 5 orders of magnitude lower than the value of the ionic conductivity. The ratio between the ionic and electronic conductivity of Ta-LLZO meets the requirements for materials for the development of solid-state devices based on them.

CONCLUSION

The possibility of obtaining high-density ceramics (~97–98%) by spark plasma sintering (SPS) from powders of cubic modification of solid electrolytes Al-LLZO and Ta-LLZO with a garnet structure under optimal processing conditions (sintering temperature 1000–1100 °C, molding pressure 50 MPa, sintering duration 10–15 min) is shown. The SPS process is an effective technology for compaction of cubic modification of Al- and Ta-substituted $Li_7La_3Zr_2O_{12}$.

It has been established that during the SPS process there is no change in the phase composition of the Al-LLZO and Ta-LLZO samples and the formation of nonconducting impurity phases.

Total ionic conductivity ($\sigma_{total} = 4–6\times10^{-4}$ S/cm) and electron conductivity (at the level of 10^{-9} S/cm) are achieved for single-phase LLZO samples free of impurity phases (La_2O_3, ZrO_2, $La_2Zr_2O_7$) with a maximum density (97–98%). The characteristics of Al-LLZO and Ta-LLZO ceramics consolidated by the SPS method correspond to the characteristics of the products of leading companies in the field of commercialization of solid electrolytes [28].

FUNDING

The work was carried out within the framework of the state assignment of the Ministry of Science and Higher Education of the Russian Federation, topic FMEZ-2022–0015 and topic FZNS-2023–0003 (regarding the synthesis of ceramics using the SPS technology).

CONFLICT OF INTEREST

The authors declare that they have no conflict of interest.

REFERENCES

1. Yaroslavtsev, A.B., Solid electrolytes: main prospects of research and development, *Russ. Chem. Rev.*, 2016, vol. 85, no. 11, p. 1255. DOI: 10.1070/RCR4634
2. Zhao, J., Wang, X., Wei, T., Zhang, Z., Liu, G., Yu, W., Dong, X., and Wang, J., Current challenges and perspectives of garnet-based solid-state electrolytes, *J. Energy Storage*, 2023, vol. 68, 107693. https://doi.org/10.1016/j.est.2023.107693
3. Han, Y., Chen, Y., Huang, Y., Zhang, M., Li, Z., and Wang, Y., Recent progress on garnet-type oxide electrolytes for all-solid-state lithium-ion batteries, *Ceram. Int.,* 2023, vol. 49, p. 29375. https://doi.org/10.1016/j.ceramint.2023.06.153
4. Kundu, S., Kraytsberg, A., and Ein-Eli, Y., Recent development in the field of ceramics solid-state electrolytes: I–oxide ceramic solid-state electrolytes, *J. Solid State Electrochem.*, 2022, vol. 26, p. 1809.
5. Kunshina, G.B., Ivanenko, V.I., and Bocharova, I.V., Synthesis and Study of Conductivity of Al-Substituted $Li_7La_3Zr_2O_{12}$, *Russ. J. Electrochem.*, 2019, vol. 55, p. 558. DOI: 10.1134/S1023193519060132

6. Kunshina, G.B., Bocharova, I.V., and Shcherbina, O.B., Electrical Conductivity and Mechanical Properties of $Li_{7-3x}Al_xLa_3Zr_2O_{12}$ Solid Electrolyte, *Inorg. Mater.,* 2022, vol. 58, no. 2, p. 147. DOI: 10.1134/S0020168522020091
7. Kunshina, G.B., and Bocharova, I.V., Specific Features of the Formation of Cubic Al-substituted $Li_7La_3Zr_2O_{12}$, *Russ. J. Appl. Chem.*, 2022, vol. 95, no. 6, p. 789. DOI: 10.1134/S1070427222060039
8. Druzhinin, K.V., Shevelin, P.Yu., and Il'ina, E.A., Cycling Performance at $Li_7La_3Zr_2O_{12}$ |Li Interface, *Russ. J. Appl. Chem.,* 2018, vol. 91, p. 63. https://doi.org/10.1134/S107042721801010X
9. Han, F., Westover, A.S., Yue, J., Fan, X., Wang, F., Chi, M., Leonard, D.N., Dudney, N.J., Wang, H., and Wang, C., High electronic conductivity as the origin of lithium dendrite formation within solid electrolytes, *Nature Energy*, 2019, vol. 4, p. 187.
10. Cheng, L., Wu, C.H., Jarry, A., Chen, W., Ye, Y., Zhu, J., Kostecki, R., Persson, K., Guo, J., Salmeron, M., Chen, G., and Doeff, M., Interrelationships among Grain Size, Surface Composition, Air Stability, and Interfacial Resistance of Al-Substituted $Li_7La_3Zr_2O_{12}$ Solid Electrolytes, *ACS Appl. Mater. & Interfaces,* 2015, vol. 7(32), p. 17649.
11. Sharafi, A., Yu, S., Naguib, M., Lee, M., Ma, C., Meyer, H.M., Nanda, J., Chi, M., Siegel, D.J., and Sakamoto, J., Impact of air exposure and surface chemistry on Li-$Li_7La_3Zr_2O_{12}$ interfacial resistance, *J. Mater. Chem. A.,* 2017, vol. 5, p. 13475.
12. Xia, W., Xu, B., Duan, H., Tang, X., Guo, Y., Kang, H., Li, H., and Liu, H., Reaction mechanisms of lithium garnet pellets in ambient air: The effect of humidity and CO_2, *J. Amer. Ceram. Soc.,* 2017, vol. 100, issue 7, p. 2832.
13. Kobi, S., and Mukhopadhyay, A., Structural (in) stability and spontaneous cracking of Li-La-zirconate cubic garnet upon exposure to ambient atmosphere, *J. Eur. Ceram. Soc.,* 2018, vol. 38, p. 4707.
14. Waetzig, K., Heubner, C., and Kusnezoff, M., Reduced Sintering Temperatures of Li^+ Conductive $Li_{1.3}Al_{0.3}Ti_{1.7}(PO_4)_3$ Ceramics, *Crystals,* 2020, vol. 10, p. 408. DOI: 10.3390/cryst10050408
15. Vinnichenko, M., Waetzig, K., Aurich, A., Baumgaertner, C., Herrmann, M., Ho, C.W., Kusnezoff M., and Lee, C.W., Li-Ion Conductive $Li_{1.3}Al_{0.3}Ti_{1.7}(PO_4)_3$ (LATP) Solid Electrolyte Prepared by Cold Sintering Process with Various Sintering Additives, *Nanomaterials*, 2022, vol. 12, p. 3178. https://doi.org/10.3390/nano12183178
16. Shichalin, O.O., Belov, A.A., Zavyalov, A.P., Papynov, E.K., Azon, S.A., Fedorets, A.N., Buravlev, I.Yu, Balanov, M.I., Tananaev, I.G., Qian, Zhang, Yun, Shi, Mingjun, Niu, Wentao, Liu, and Portnyagin, A.S., Reaction synthesis of $SrTiO_3$ mineral-like ceramics for strontium-90 immobilization via additional in-situ synchrotron studies, *Ceram. Int.,* 2022, vol. 48, iss. 14, p. 19597. https://doi.org/10.1016/j.ceramint.2022.03.068
17. Papynov, E.K., Shichalin, O.O., Buravlev, I.Yu., Belov, A.A., Portnyagin, A.S., Fedorets, A.N., Azarova, Yu.A., Tananaev, I.G., and Sergienko, V.I., Spark plasma sintering-reactive synthesis of $SrWO_4$ ceramic matrices for ^{90}Sr immobilization, *Vacuum*, 2020, vol. 180, p. 109628.
18. Kotobuki, M. and Koishi, M., High conductive Al-free Y-doped $Li_7La_3Zr_2O_{12}$ prepared by spark plasma sintering, *J. Alloys Compd.*, 2020, vol. 826, p. 154213.
19. Baek, S.-W., Lee, J.-M., Young Kim, T., Song, M.-S., and Park, Y., Garnet related lithium ion conductor processed by spark plasma sintering for all solid state batteries, *J. Power Sources*, 2014, vol. 249, p. 197. http://dx.doi.org/10.1016/j.jpowsour.2013.10.089
20. Yamada, H., Ito, T., and Basappa, R.H., Sintering Mechanisms of High-Performance Garnet-type Solid Electrolyte Densified by Spark Plasma Sintering, *Electrochim. Acta*, 2016, vol. 222, p. 648. http://dx.doi.org/10.1016/j.electacta.2016.11.020
21. Xue, J., Zhang, K., Chen, D., Zeng, J., and Luo, B., Spark plasma sintering plus heat-treatment of Ta-doped $Li_7La_3Zr_2O_{12}$ solid electrolyte and its ionic conductivity, *Mater. Res. Express*, 2020, vol. 7, p. 025518. https://doi.org/10.1088/2053–1591/ab7618
22. Abdulai, M., Dermenci, K.B., and Turan, S., SPS sintering and characterization of $Li_7La_3Zr_2O_{12}$ solid electrolytes, *MRS Energy Sustain.*, 2023, vol. 10, p. 94. https://doi.org/10.1557/s43581–022–00055–7
23. Kunshina, G.B., Shichalin, O.O., Belov, A.A., Papynov, E.K., Bocharova, I.V., and Shcherbina, O.B., Properties of $Li_{1.3}Al_{0.3}Ti_{1.7}(PO_4)_3$ Lithium-Conducting Ceramics Synthesized by Spark Plasma Sintering, *Russ. J. Electrochem.*, 2023, vol. 59, p. 173. DOI: 10.1134/S1023193523030060
24. Tezuka, T., Inagaki, Y., Kodama, S., Takeda, H., and Yanase, I., Spark plasma sintering and ionic conductivity of $Li_{1.3}Al_{0.3}Ti_{1.7}(PO_4)_3$ fine particles synthesized by glass crystallization, *Powder Technology,* 2023, vol. 429, p. 118870. https://doi.org/10.1016/j.powtec.2023.118870
25. Kunshina, G.B., Bocharova, I.V., and Kalinkin, A.M., Optimization of LLZO solid electrolyte transition from tetragonal modification into cubic one using mechanical activation, *Inorg. Mater.,* 2024, vol. 60, no.1, pp. 111-119
26. Bocharova, I.V., Kunshina, G.B., and Efremov, V.V., Synthesis and Study of Electrochemical Characteristics of Ta-doped Solid Electrolyte $Li_7La_3Zr_2O_{12}$, *Tr. Kolsk. nauchn. tsentra RAN. Ser. Tekh. nauki*, (in Russian), 2023, vol. 14, no 3, p. 54.
27. Charrad, G., Pradeilles, S., Taberna, P.-L., Simon, P., and Rozier, P., Investigation of Chemical and Thermal Stability of $Li_{7-x}La_3Zr_{2-x}Ta_xO_{12}$ Garnet Type Solid-State Electrolyte to Assemble Self-

Standing Li-based All Solid-State Battery, *Energy Technol.,* 2023, vol. 11, 2300234.

28. https://www.msesupplies.com
29. Irvin, J.T.S., Sinclair, D.C., and West, A.R., Electroceramics: Characterization by Impedance Spectroscopy, *Adv. Mater.,* 1990, vol. 2, no. 3, p. 132.
30. Xue, W., Yang, Y., Yang, Q., Liu, Y., Wang, L., Chen, C., and Cheng, R., The effect of sintering process on lithium ionic conductivity of $Li_{6.4}Al_{0.2}La_3Zr_2O_{12}$ garnet produced by solid-state synthesis, *RSC Adv.,* 2018, vol. 8, p. 13083. DOI: 10.1039/c8ra01329b
31. Kotobuki, M., Munakata, H., Kanamura, K., Sato, Y., and Yoshida, T., Compatibility of $Li_7La_3Zr_2O_{12}$ Solid Electrolyte to All-Solid-State Battery Using Li Metal Anode, *J. Electrochem. Soc.,* 2010, vol. 157 (10), A1076. DOI: 10.1149/1.3474232
32. Zhang, Y., Chen, F., Tu, R., Shen, Q., and Zhang, L., Field assisted sintering of dense Al-substituted cubic phase $Li_7La_3Zr_2O_{12}$ solid electrolytes, *J. Power Sources*, 2014, vol. 268, p. 960.
33. Dong, Z., Xu, C., Wu, Y., Tang, W., Song, S., Yao, J., Huang, Z., Wen, Z., Lu, L., and Hu, N., Dual Substitution and Spark Plasma Sintering to Improve Ionic Conductivity of Garnet $Li_7La_3Zr_2O_{12}$, *Nanomaterials,* 2019, vol. 9, p. 721. DOI: 10.3390/nano9050721
34. Salimkhani, H., Yurum, A., and Gursel, S.A., A glance at the influence of different dopant elements on $Li_7La_3Zr_2O_{12}$ garnets, *Ionics,* 2021, vol. 27, p. 3673. https://doi.org/10.1007/s11581−021−04152−4
35. Zhu, Y., Zhang, J., Li, W., Zeng, Y., Wang, W., Yin, Z., Hao, B., Meng, Q., Xue, Y., Yang, J., and Li, S., Enhanced Li^+ conductivity of $Li_7La_3Zr_2O_{12}$ by increasing lattice entropy and atomic redistribution via Spark Plasma Sintering, *J. Alloys Compd.*, 2023, vol. 967, p. 171666.
36. Hoinkis, N., Schuhmacher, J., Leukel, S., Loho, C., Roters, A., Richter, F.H., and Janek, J., Particle Size-Dependent Degradation Kinetics of Garnet-Type $Li_{6.5}La_3Zr_{1.5}Ta_{0.5}O_{12}$ Solid Electrolyte Powders in Ambient Air, *J. Phys. Chem. C.,* 2023, vol. 127 (17), p. 8320. https://doi.org/10.1021/acs.jpcc.3c01027
37. Yi, M., Liu, T., Wang, X., Li, J., Wang, C., and Mo, Y., High densification and Li-ion conductivity of Al-free $Li_{7-x}La_3Zr_{2-x}Ta_xO_{12}$ garnet solid electrolyte prepared by using ultrafine powders, *Ceram. Int.*, 2019, vol. 45, p. 786. https://doi.org/10.1016/j.ceramint.2018.09.245